Journal of Power Sources 195 (2010) 6172–6176

Contents lists available at ScienceDirect

Journal of Power Sources

journal homepage: www.elsevier.com/locate/jpowsour

Short communication

Carbon anode for dry-polymer electrolyte lithium batteries

D. Saito, Y. Ito, K. Hanai, T. Kobayashi, N. Imanishi*, A. Hirano, Y. Takeda, O. Yamamoto

Department of Chemistry, Faculty of Engineering, Mie University, 1577 Kurimamachia-cho, Tsu, Mie 514-8507, Japan

ARTICLE INFO

Article history:
Received 20 September 2009
Received in revised form
18 November 2009
Accepted 19 November 2009
Available online 24 November 2009

Keywords:
Polymer electrolyte
Lithium battery
Graphite anode
Safety

ABSTRACT

A spherical carbon material of meso-carbon microbead (MCMB) was examined as an anode in a polyethylene oxide (PEO) based polymer electrolyte lithium battery. The electrochemical performance of the carbon electrode with the polymer electrolyte depended on the electrode thickness and the particle size of MCMB. The 30 μm-thick electrode of MCMB with the particle size of 20–30 μm showed a reversible capacity comparable with that in a liquid electrolyte, but the 100 μm-thick electrode showed a half of the 30 μm-thick electrode. The smaller particle size of 5–8 μm exhibited a high irreversible capacity at the first charge–discharge cycle. The reaction heat between MCMB and the polymer electrolyte was 0.5 J mAh^{-1}, which was much lower compared to those between lithium metal and the polymer electrolyte, 1.2 J mAh^{-1}, and MCMB and conventional liquid electrolyte, 4.3 J mAh^{-1}.

1. Introduction

Dry-polymer electrolyte lithium secondary batteries have been extensively studied for three decades, because these batteries are expected to overcome the safety problem, the energy density, and the cost of conventional liquid electrolyte systems. Previously developed polymer electrolyte lithium batteries have mainly used a lithium metal anode and oxide cathode [1]. Although lithium metal can achieve a high energy density, it has safety problems arising from a dendrite formation on the anode surface [2] and a high reaction heat with other cell components [3]. The large-size lithium batteries using polymer electrolyte and lithium anode for telecommunication stations in Houston, USA, exploded and burst into flame in 2006. Therefore, an alternative anode for the lithium polymer battery should be developed. Investigations of alternative anode for the lithium metal anode over the last two decades have revealed that lithium alloys, transition metal oxides, and lithium transition metal nitrides become a promising candidate for their large reversible capacity and the low redox potential. It is the major problem that lithium alloys generally undergo several phase changes during the charge and discharge cycles, which are accompanied by severe volume expansion and contraction [4]. The transition metal oxides show a large irreversible capacity during the first charge process [5]. A major hindrance about lithium transition metal nitrides is that they possess a large amount of lithium in the structure, which must be extracted from the nitrides in the first anodic oxidation. Therefore, the nitride anodes cannot be directly combined with typical high potential cathodes such as $LiCoO_2$ and $LiMn_2O_4$ [6]. The reversible capacity of graphite was lower than those of lithium alloys and transition metal oxides, but graphite showed an excellent electrochemical performance in an ethylene carbonate based electrolyte. Therefore, graphite and related carbon materials have been widely used as the anode in the lithium-ion batteries. However, it is commonly recognized that the cyclic performance of the graphite anode with the polymer electrolyte is quite poor because of a poor electrochemical compatibility between the carbon and the polymer electrolyte. In the previous paper [7], we have reported that meso-carbon microbead (MCMB) showed an excellent electrochemical performance with polyethylene (PEO) based polymer electrolyte. And also, Kobayashi et al. reported an excellent performance of the spherical natural graphite anode in the polymer electrolyte cell. The reversible capacities of 360 mAh g^{-1} at the first cycle and 300 mAh g^{-1} at the 250th cycle were observed [8]. These results suggest that the compatibility of the spherical graphite with the PEO-based polymer electrolyte is practically high enough, but the interface characteristics between the graphite and the polymer electrolyte are not clear. In this study, the electrode performances of the MCMB anode with the PEO-based electrolyte have been examined as a function of the particle size and the electrode thickness. The interface resistance between the polymer electrolyte and the carbon anode has been measured to discuss the electrochemical performance. The reaction heat between MCMB and the polymer electrolyte was compared with those between lithium metal and the polymer electrolyte, and MCMB and conventional liquid electrolyte.

* Corresponding author. Tel.: +81 59 231 9420; fax: +81 59 231 9478.
E-mail address: imanishi@chem.mie-u.ac.jp (N. Imanishi).

0378-7753/$ – see front matter © 2009 Elsevier B.V. All rights reserved.
doi:10.1016/j.jpowsour.2009.11.076

2. Experimental

Two different particle sizes of MCMB (Osaka Gas Chemicals Co. Ltd, Japan, 5–8 μm and 20–30 μm) were used as spherical graphite materials. The composite anode with the polymer electrolyte was prepared as follows. $Li(CF_3SO_2)_2N$ (Fluka) was dissolved into anhydrous acetonitrile (AN), and MCMB and a vapor grown carbon fiver (VGCF, Showa Denko, Japan), 0.15 μm in diameter and 20 μm in length were added into the solution. And then, PEO (Aldrich, $Mw = 6 \times 10^5$) was dissolved and stirred for 3 h. The ratio of MCMB, VGCF, $Li(CF_3SO_2)_2N$ and PEO was 25:5:5:15 in weight. In some cases, nano-size $BaTiO_3$ (Aldrich, average particle size of 0.1 μm) was added into the slurry. The anode slurry was spread on a copper foil using a coating machine. The thickness of the electrode was controlled by the slurry viscosity and the coating height. For example, the viscosity was adjusted to be 5000–8000 cP to have the thickness of 30 μm of the final product. The coated electrode was dried at 120 °C under vacuum for 3 h to remove AN completely, and finally pressured to make a sure contact in the whole system.

The polymer electrolyte sheet was prepared by the previously reported method [9]. A given weight of PEO ($Mw = 6 \times 10^5$) and $Li(CF_3SO_2)_2N$ (Li/O = 1/18) with 10 wt% $BaTiO_3$ were added into AN. After strong stirring over night, the viscous solution was cast in a Teflon dish. After AN was slowly and completely evaporated, the obtained film was further dried at 90 °C under vacuum for 8 h. The electrical conductivity of the obtained polymer electrolyte was about 5×10^{-4} S cm^{-1} at 60 °C, which is comparable to the previously reported value [10].

The electrode performance was examined using a lamination-type cell. A stack of the graphite electrode cast on a copper foil current collector, polymer electrolyte, and lithium metal counter electrode with a copper foil current collector was sandwiched between glass plates. The cell was packed in an aluminum-laminate envelope. The active area of the electrode was 2.25 cm^2 and the thickness of the polymer electrolyte was adjusted to be 200 μm by a polyethylene spacer. The cells were galvanostatically charged and discharge in the voltage range of 0.01–1.5 V using a Nagano BTS 2004H battery cycler. The charge and discharge rates were normally set at C/10. The operation temperature was 60 °C, because the conductivity of the polymer electrolyte below 55 °C was too low to apply a high current density.

Impedance measurements were performed using a Solartron 1260 frequency analyzer with a Solartron 1286 electrochemical interface in the frequency range of 10^5 to 0.01 Hz. The symmetrical cell, $Li_xMCMB/PEO_{18}Li(CF_3SO_2)_2N/Li_xMCMB$, was prepared using the $Li/PEO_{18}Li(CF_3SO_2)_2N/MCMB/PEO_{18}Li(CF_3SO_2)_2N/MCMB/PEO_{18}Li(CF_3SO_2)_2N/Li$ cell. The Li and the MCMB electrodes were electrically connected for over night to insert lithium into MCMB. Differential scanning calorimetry (DSC) measurements were carried out under an Ar gas flow using a Rigaku Thermo Plus 8330, and Al_2O_3 was used as the reference. The samples were packed in a stainless steel pan and the temperature scanning rate was 5 °C min^{-1}.

3. Results and discussion

Typical charge (lithium insertion into MCMB) and discharge (lithium extraction from lithiated MCMB) curves and cyclic performances at 60 °C and at a rate of C/10 for the $Li/PEO_{18}Li(CF_3SO_2)_2N/MCMB$ (particle size of 20–30 μm) cells with different thickness of the MCMB anodes are shown in Fig. 1. The reversible capacity of 310 mAh g^{-1} at the second cycle for the 30 μm-thick electrode is slightly higher than that of 280 mAh g^{-1} reported previously [7]. The high reversible capacity observed in this study may be due to the use of VGCF in place of acetylene

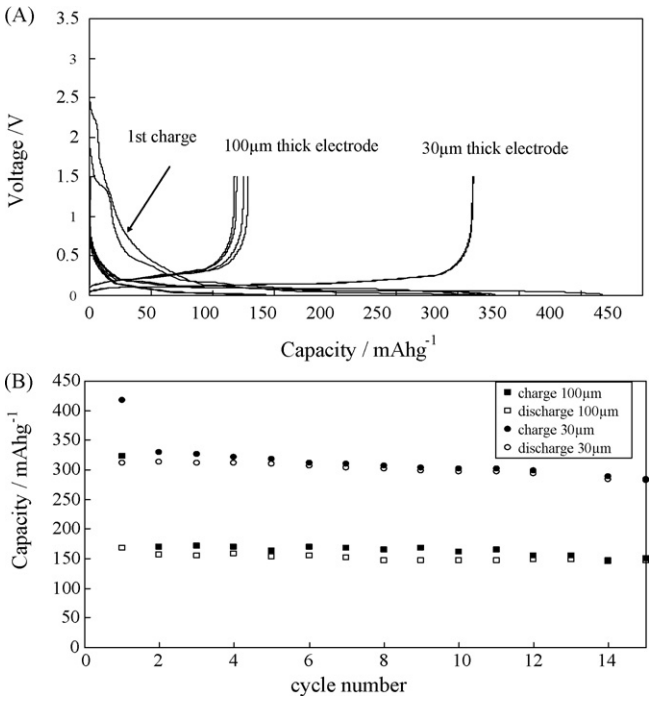

Fig. 1. Charge and discharge curves (A) and cycling performance (B) at 60 °C and at C/10 rate for the $Li/PEO_{18}Li(CF_3SO_2)_2N/MCMB$ (particle size of 20–30 μm) cell with about 30 and 100 μm-thick MCMB electrode.

black in the electrode composite. VGCF was more effective as a conductive additive for the electrode in the polymer electrolyte cell. This composite with VGCF showed stable reversible capacity of 350 mAh g^{-1} in the liquid electrolyte of 1 M $LiClO_4$ in ethylene carbonate and diethyl carbonate (50:50 vol.%) as shown in Fig. 2. On the other hand, the 100 μm-thick MCMB anode shows a specific reversible capacity as low as 150 mAh g^{-1}. The first irreversible capacity of about 170 mAh g^{-1} for this thicker electrode is higher than that of 100 mAh g^{-1} for the 30 μm-thick one. The irreversible capacity corresponds to the formation of a solid electrolyte interface (SEI) on the graphite surface, which prevents the further reaction of the polymer electrolyte and graphite [11]. The higher irreversible capacity for the thicker electrode could be explained by higher contact area of MCMB and the polymer electrolyte.

The interface resistance between the carbon electrode and the polymer electrolyte was measured using impedance analysis. Fig. 3 shows the impedance profiles for the cell, $Li/PEO_{18}Li(CF_3SO_2)_2N/MCMB$ (20–30 μm) with the thickness of 30 μm, where the measurements were done at 60 °C after 10 cycles and at the anode potentials of about 600 mV (discharged state) and

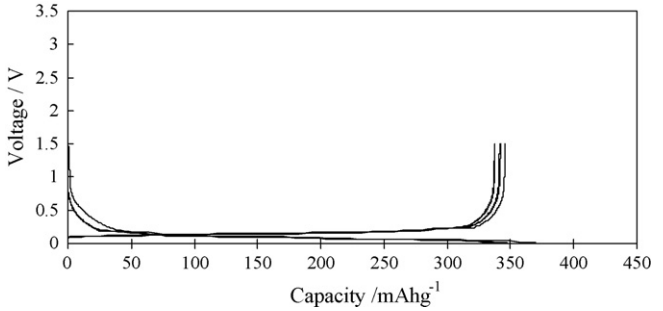

Fig. 2. Charge and discharge curves of the composite anode in the liquid electrolyte cell. The electrode is consisted of 80 wt% of MCMB, 10 wt% of VGCF and 10 wt% of polyvinylidene fluoride (PVdF).

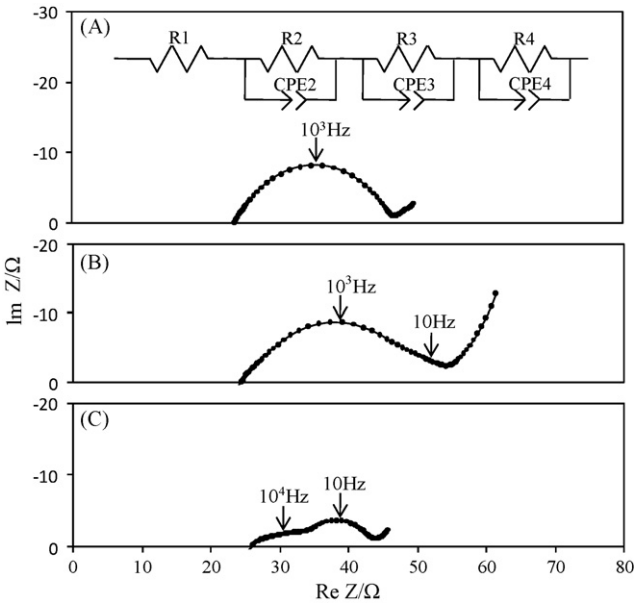

Fig. 3. Impedance profiles of the Li/$PEO_{18}Li(CF_3SO_2)_2N$/MCMB (20–30 μm) cell with about 30 μm-thick MCMB electrode at the electrode potentials of 60 mV (A) and 600 mV (B) vs. Li/Li^+, with that of Li_xMCMB/$PEO_{18}Li(CF_3SO_2)_2N/Li_x$MCMB symmetrical cell (C). The impedance spectra of (A) and (B) were measured after 10 cycles.

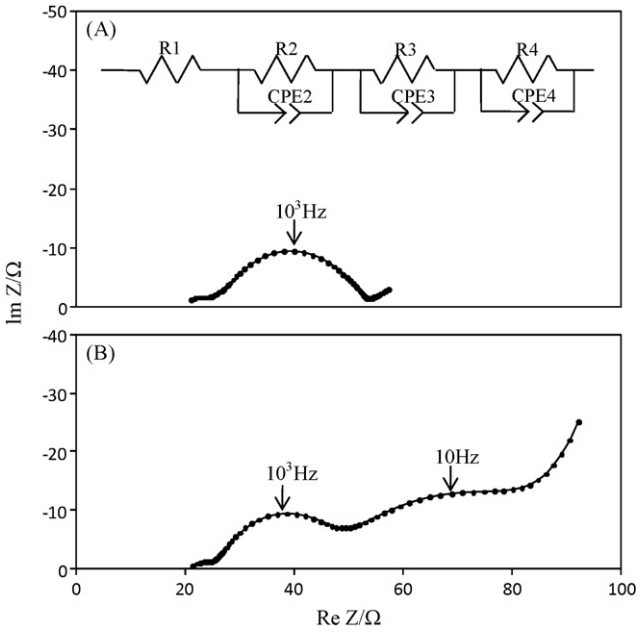

Fig. 4. Impedance profiles of the Li/$PEO_{18}Li(CF_3SO_2)_2N$/MCMB (20–30 μm) cell with about 100 μm-thick MCMB electrode at the electrode potentials of 60 mV (A) and 600 mV (B) vs. Li/Li^+ at 60 °C. The impedance spectra of (A) and (B) were measured after 10 cycles.

60 mV (charged state). The impedance spectrum at 60 mV shows a semicircle and the one at 600 mV appears to be a diminished semicircle. The intercept of the semicircle with a real axis at a high frequency corresponds to the ohmic resistance, which is predominantly the bulk resistance of the polymer electrolyte [12]. The electrolyte bulk resistance (R_1), the electrolyte grain boundary resistance (R_2), the interfacial resistance between Li metal and the polymer electrolyte (R_3), and the interfacial resistance between MCMB and the polymer electrolyte (R_4) were estimated using an equivalent circuit shown in Fig. 3. The fitted values for the spectrum at 600 mV were $R_1 = 25\,\Omega$, $R_2 = 2.0\,\Omega$, $R_3 = 16.7\,\Omega$, and $R_4 = 10.6\,\Omega$. For the cell at 60 mV, $R_1 = 24\,\Omega$, $R_2 = 0.5\,\Omega$, and $R_3 = 22.2\,\Omega$. R_4 was too small for the accurate estimation. R_1 and R_2 are similar to those obtained from the Cu/$PEO_{18}Li(CF_3SO_2)_2N$/Cu cell. R_3 values are similar for the both cells and comparable to that obtained for the Li/$PEO_{18}Li(CF_3SO_2)_2N$/Li. R_4 at 60 mV is much lower than that at 600 mV. These results suggest that R_4 corresponds to the charge transfer resistance between MCMB and the polymer electrolyte, and the magnitude depends on the lithium content of MCMB. The assignment of R_4 is also supported by the fact that the interface resistance observed in the Li_xMCMB/$PEO_{18}Li(CF_3SO_2)_2N/Li_x$MCMB symmetrical cell (C) is estimated to be 10.3 Ω. This is similar to the R_4 obtained for the half-cell (B) at 600 mV.

Fig. 4 shows impedance profiles for the cell, Li/$PEO_{18}Li(CF_3SO_2)_2N$/MCMB (20–30 μm) with a thickness of about 100 μm, charged at 60 and 600 mV and measured at 60 °C after 10 cycles. The impedance profile for the cell at 60 mV is identical to that observed for the cell with the 30 μm-thick MCMB electrode. On the other hand, the cell at 600 mV was analyzed using the equivalent circuit shown in the figure as $R_1 = 22\,\Omega$, $R_2 = 4\,\Omega$, $R_3 = 20\,\Omega$, and $R_4 = 58\,\Omega$. R_1, R_2, and R_3 are comparable to those for the cell with the 30 μm-thick MCMB electrode. However, R_4 is three times higher than that for the cell with the 30 μm-thick MCMB electrode. The low reversible capacity of the cell with the 100 μm-thick MCMB electrode could be explained by the high cell resistance in the discharged state at 600 mV. This assumption was confirmed by the result that the reversible capacity was enhanced at low charge and discharge current densities. The reversible capacity of 100 mAh g^{-1} at the C/10 rate for the cell with the 100 μm-thick MCMB anode increased to 290 mAh g^{-1} at the C/20 rate as shown in Fig. 5. The 30 μm-thick MCMB electrode composed of particles of 20–30 μm corresponds to one particle layer, while the 100 μm-thick electrode has about three stacked layers of MCMB particles. The contact resistance between MCMB particles and between MCMB and VGCF may result in high R_4 resistance in the latter electrode.

Figs. 6 and 7 show charge–discharge curves and cycle performances of the Li/$PEO_{18}Li(CF_3SO_2)_2N$/MCMB (particle size of 5–8 μm) cells with 30 and 10 μm-thick MCMB electrodes, respectively. The reversible capacity of 270 mAh g^{-1} was obtained for the cell with 10 μm-thick MCMB electrode. However, a high irreversible capacity was also observed at the first cycle and the coulomb efficiency becomes about 67%. The irreversible capacity is due to the reaction of the polymer electrolyte and the MCMB electrode. The amount of the reaction product (SEI) depends on the contact area between the polymer electrolyte and the carbon anode. The cell with 30 μm-thick electrode shows a lower irreversible capacity compared to the 10 μm-thick electrode. The impedance profiles for the Li/$PEO_{18}Li(CF_3SO_2)_2N$/MCMB (particle

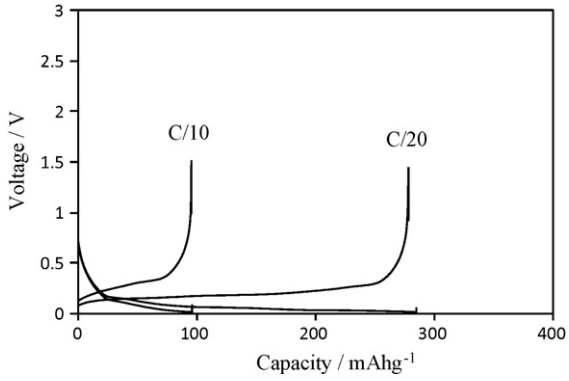

Fig. 5. Charge–discharge curves of the Li/$PEO_{18}Li(CF_3SO_2)_2N$/MCMB (20–30 μm) cell with about 100 μm-thick MCMB electrode at C/10 rate (A) and C/20 rate (B) at 60 °C.

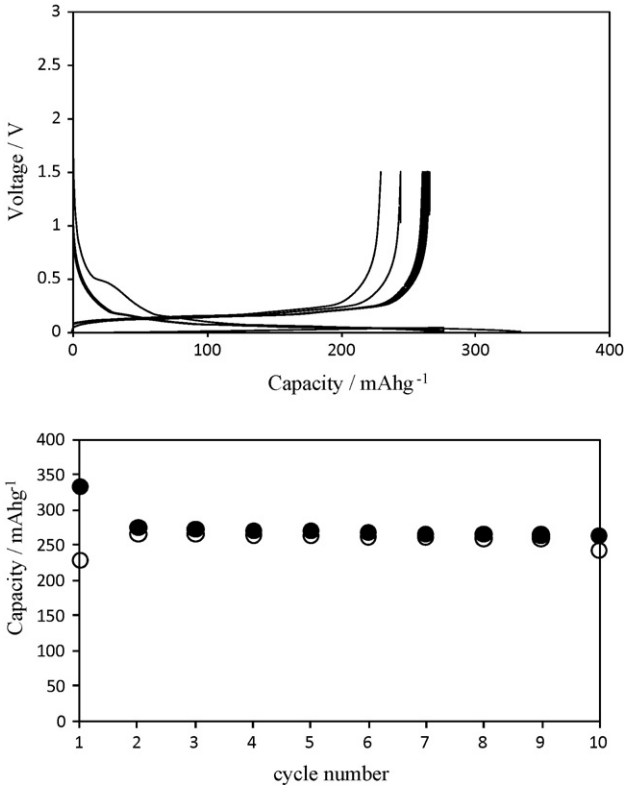

Fig. 6. Charge–discharge curves and cycling performance at 60 °C and at C/10 rate of the Li/$PEO_{18}Li(CF_3SO_2)_2N$/MCMB (particle size of 5–8 μm) cell with about 30 μm-thick MCMB electrode.

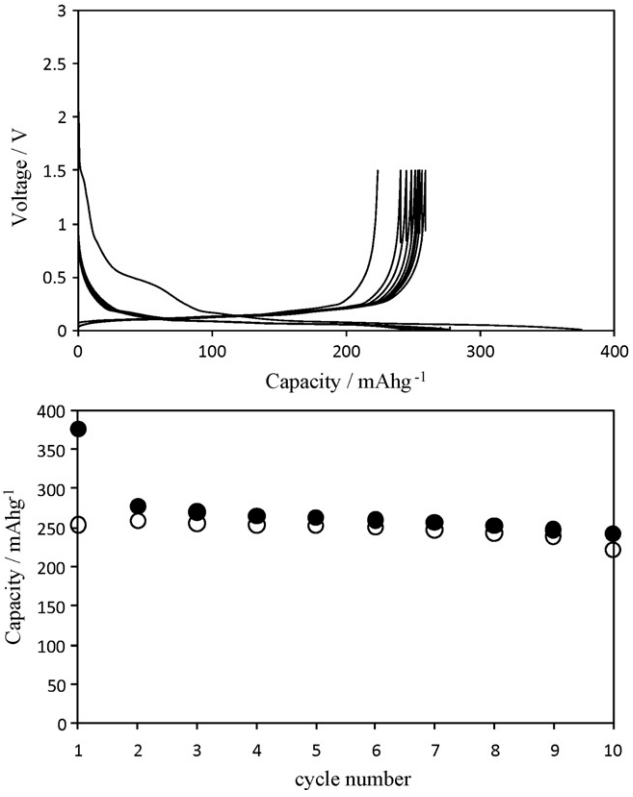

Fig. 7. Charge–discharge curves and cycling performance at 60 °C and at C/10 rate for the Li/$PEO_{18}Li(CF_3SO_2)_2N$/MCMB (particle size of 5–8 μm) cell with about 10 μm-thick MCMB electrode.

size of 5–8 μm) cell with 30 μm-thick electrode at 60 °C showed a similar profile to that of the cell with 30 μm-thick MCMB electrode (particle size of 20–30 μm). These results explain that the high contact resistance between MCMB particles may be compensated by the large surface area of the small size MCMB particles. In the 100 μm-thick MCMB electrode, however, the contact resistance becomes more dominant and leads to a low reversible capacity of 100 mAh g^{-1}.

The stability of the MCMB anode/polymer electrolyte interface is one of the most important parameter in terms of battery cyclability. Many reports indicate that lithium is passivated in PEO-based electrolytes with growth of a resistive layer at the interface, although the mechanism and the nature of the passivation process are not completely clarified [13]. Stability of the lithium/polymer electrolyte interface may be related with its affinity to water. Finely dispersed ceramic particles may trap water and other solvents, thus progressively remove impurities from the interface that are considered to be the major cause for passivation of the lithium metal electrode [14]. The interface resistance of Li/$PEO_{10}Li(CF_3SO_2)_2N$ is improved by addition of 10 wt% of Al_2O_3 (1 μm), TiO_2 (1 μm) and $BaTiO_3$ (0.1 μm) [15]. In this study, the effect of $BaTiO_3$ (particle size of 0.1 μm) addition into MCMB composite anode was examined. In Fig. 8, the cycle performances of the Li/$PEO_{18}Li(CF_3SO_2)_2N$/MCMB (particle size of 20–30 μm) with and without 10 wt% $BaTiO_3$, are compared at 60 °C and C/10 rate, where the electrode thickness was about 30 μm. Stable reversible capacity of about 350 mAh g^{-1} is observed for the MCMB anode with $BaTiO_3$, which is comparable to that for the cell using a liquid electrolyte. The first cycle charge–discharge efficiency is 77%, which is slightly improved by addition of $BaTiO_3$ from 75% obtained for the anode without $BaTiO_3$. These results suggest that the addition of $BaTiO_3$ into carbon anode is quite effective to obtain a high energy density of lithium polymer electrolyte batteries.

The safety of small-size lithium-ion batteries for conventional applications is well established. In contrast, the safety of large-size

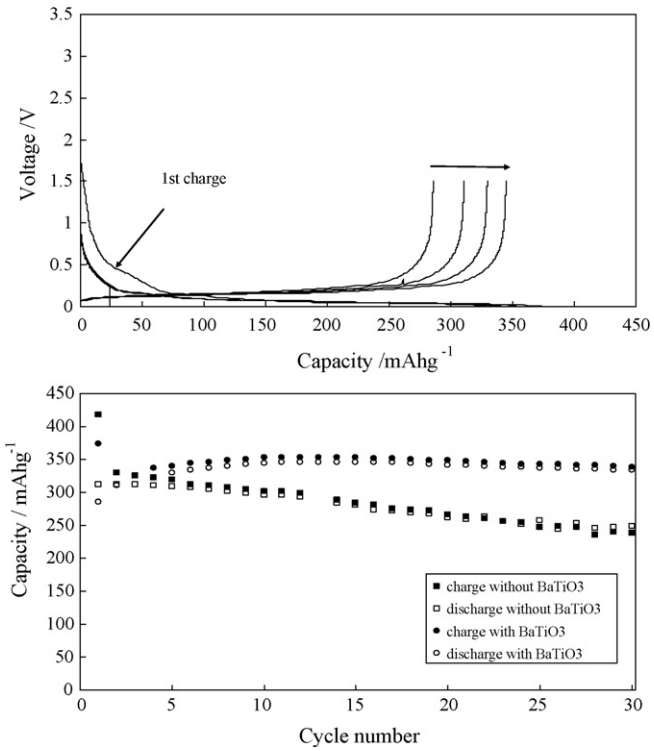

Fig. 8. Cycling performance for the Li/$PEO_{18}Li(CF_3SO_2)_2N$/MCMB (particle size of 20–30 μm) cell with 10 wt% $BaTiO_3$ at 60 °C and at C/10 rate. The electrode thickness was about 30 μm.

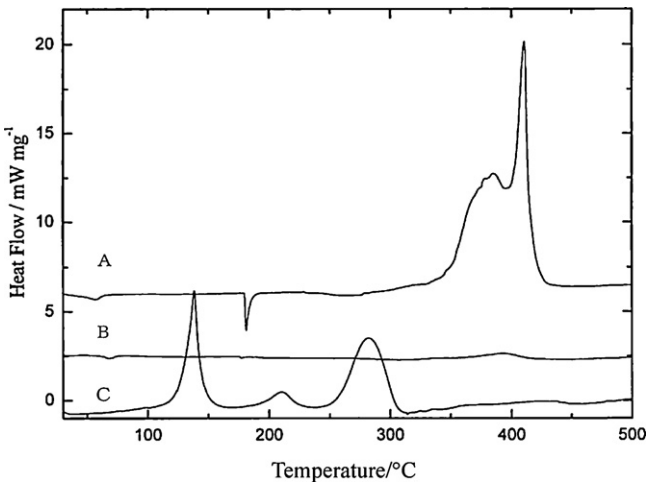

Fig. 9. DSC curves of (A) Li and $PEO_{18}Li(CF_3SO_2)_2N$, (B) MCMB and $PEO_{18}Li(CF_3SO_2)_2N$, and (C) MCMB and EC-DMC-$LiPF_6$.

lithium-ion batteries is still questionable, especially in case of abusive use. The safety of lithium-ion batteries is mainly related to the thermal reactivity of the components. Fig. 9 shows differential scanning calorimetry (DSC) curves for the charged composite MCMB anode mixed with the PEO electrolyte, Li metal with the PEO electrolyte (1:1 weight ratio), and charged MCMB with the liquid electrolyte of $LiPF_6$ in ethylene carbonate and dimethyl carbonate (1:1 volume ratio). The MCMB and $PEO_{18}Li(CF_3SO_2)_2N$ composite anode shows the lowest specific reaction heat of 160 J g^{-1}. The reaction heat should be compared in terms of the heat per discharge capacity, i.e., J mAh^{-1}. The value of 160 J g^{-1} for the MCMB anode corresponds to 0.5 J mAh^{-1}. The reaction heats of other samples are 4600 J g^{-1} and 1.24 J mAh^{-1} for Li metal with PEO and 1500 J g^{-1} and 4.3 J mAh g^{-1} for MCMB with the liquid electrolyte. Much lower reaction heat of the MCMB electrode with the PEO-based polymer electrolyte is quite attractive as the anode for large scale lithium-ion batteries.

4. Conclusions

To develop less flammable lithium-ion battery, the carbon anode for the dry-polymer electrolyte lithium battery has been examined. The composite anode of spherical mesocarbon microbead (MCMB), VGCF, and $PEO_{18}Li(CF_3SO_2)_2N$-$BaTiO_3$ showed an excellent electrochemical performance when used with $PEO_{18}Li(CF_3SO_2)_2N$-$BaTiO_3$ electrolyte. The performance depended on the thickness of the electrode. The 100 μm-thick electrode of the MCMB with the particle size of 20–30 μm showed a low reversible capacity at high current density. The low capacity could be explained by the high charge transfer resistance at the discharged state. The smaller particle size of 5–8 μm showed a large irreversible capacity at the first cycle. It was due to the reaction of MCMB and the polymer electrolyte at the first lithium insertion process and the capacity depended on the surface area of the MCMB. The low reaction heat of the MCMB and the polymer electrolyte is quite attractive to develop a safe and large dry-polymer lithium battery.

Acknowledgements

This study has been partly supported by Cooperation of Innovative Technology and Advanced Research in Evolution Area (City Area) Project of Ministry of Education, Culture, Sports, Science and Technology.

References

[1] M. Gauther, D. Fauteux, G. Vassort, A. Belanger, M. Duval, P. Ricoux, J.M. Chabagno, D. Muller, P. Rigaud, M.B. Armand, D. Deroo, J. Electrochem. Soc. 132 (1985) 1333.
[2] C. Brissot, M. Rooso, J.N. Chazalviel, S. Lascaud, J. Power Sources 81/82 (1999) 925.
[3] M.D. Farrington, J. Power Sources 96 (2001) 260.
[4] J.O. Besenhard, M. Hess, P. Komenda, Solid State Ionics 40/41 (1990) 525.
[5] P. Polzot, S. Laruelle, S. Grugeon, L. Dupon, J.-M. Tarascon, Nature 407 (2000) 496.
[6] M. Nishijima, T. Kagohashi, N. Imanishi, Y. Takeda, O. Yamamoto, S. Kondo, Solid State Ionics 83 (1996) 107.
[7] N. Imanishi, Y. Ono, K. Hanai, R. Uchiyama, Y. Liu, A. Hirano, Y. Takeda, O. Yamamoto, J. Power Sources 178 (2008) 744.
[8] Y. Kobayashi, S. Seki, Y. Mita, Y. Ohno, H. Miyashita, P. Charest, A. Guerfi, K. Zaghib, J. Power Sources 185 (2008) 542.
[9] C. Capiglia, J. Yang, N. Imanishi, A. Hirano, Y. Takeda, O. Yamamoto, J. Power Sources 119–121 (2003) 826.
[10] Q. Li, N. Imanishi, A. Hirano, Y. Takeda, O. Yamamoto, J. Power Sources 110 (2002) 38.
[11] J.O. Besenhard, M. Winter, J. Yand, W. Biberacher, J. Power Sources 54 (1995) 228.
[12] B.A. Boukamp, Solid State Ionics 20 (1986) 31.
[13] F. Copuano, F. Croce, B. Scrosati, J. Electrochem. Soc. 138 (1991) 1918.
[14] D. Fauteux, J. Electrochem. Soc. 135 (1988) 2231.
[15] Q. Li, H.Y. Sun, Y. Takeda, N. Imanishi, J. Yang, O. Yamamoto, J. Power Sources 94 (2001) 201.